Acta Crystallographica Section A
Foundations of Crystallography
ISSN 0108-7673

Received 8 April 2011
Accepted 22 April 2011

High-resolution study of (222, 113) three-beam diffraction in Ge

A. Kazimirov[a]* and V. G. Kohn[b]

[a]Cornell High Energy Synchrotron Source (CHESS), Cornell University, Ithaca, NY 14853, USA, and [b]National Research Center 'Kurchatov Institute', 123182 Moscow, Russia. Correspondence e-mail: ayk7@cornell.edu

The results of high-resolution analysis of the (222, >113) three-beam diffraction in Ge are presented. For monochromatization and angular collimation of the incident synchrotron beam a multi-crystal arrangement in a dispersive setup in both vertical and horizontal planes was used in an attempt to experimentally approach plane-wave incident conditions. Using this setup, for various azimuthal angles the polar angular curves which are very close to theoretical computer simulations for the plane monochromatic wave were measured. The effect of the strong two-beam 222 diffraction was observed for the first time with the maximum reflectivity close to 60% even though the total reflection of the incident beam into a forbidden reflection was not achieved owing to absorption. The structure factor of the 222 reflection in Ge was experimentally determined.

1. Introduction

The crystal lattice of a diamond-type structure has two interpenetrating face-centered cubic sublattices displaced by a quarter of the distance along the cube diagonal. It is well known that in monoatomic crystals (silicon, germanium, diamond) this leads to suppression of diffraction into reflections with even–even Miller indices such that $h + k + l = 4n + 2$, for example, 222. The reflections with Miller indices which are the sum of such indices of forbidden reflection and the odd–odd allowed reflections are also allowed. The suppression is complete only for spherically symmetrical atoms and very low temperatures. The real electron density in atoms inside the crystal is not fully symmetrical and some very weak diffraction may take place. That brings two questions. The first one is to determine the diffraction parameter for a weak quasi-forbidden reflection. Usually, it is defined as a structure factor F, *i.e.* an effective number of electrons in a unit cell participating in diffraction. The second interesting problem is to find the means to make such forbidden reflections stronger and the most effective way is to use multiple diffraction, in particular a three-beam diffraction, by simultaneously exciting one of the strong allowed reflections.

The second problem was solved for the first time by Renninger (1937) who applied a convenient experimental scheme in which the forbidden 222 reflection was normal to the crystal surface and satisfied the Bragg condition while the crystal was rotated around the surface normal. Then, at some azimuthal angles multiple diffraction takes place when other reflections satisfy the Bragg condition. At these crystal positions the forbidden 222 reflection becomes rather strong and can be reliably detected and studied. This setup, commonly known as a Renninger scheme, was utilized in many multiple-diffraction experiments [see the books by Authier (2005) and Chang (2004) for details] with the main emphasis given to the possibility of determining the phases of allowed reflections. Theoretical treatment based on dynamical diffraction theory of n-beam integrated intensities and comparison with experiment for the case of Ge(222/113) diffraction was given by Colella (1974). However, all experiments so far have been performed with the incident beam rather poorly collimated over both the polar and azimuth angles, and therefore the fine details in the angular dependences of the intensities of the beams participating in multiple diffraction have been washed out and lost for analysis.

This is the first problem which has been the subject of many experimental and theoretical analyses. The most detailed and extensive experimental study of the 222 diffraction in Si and Ge was performed by Roberto *et al.* (1974). The authors analyzed two mechanisms of excitation of the 222 reflection: anharmonic atomic vibrations and anticentrosymmetric valence-charge distribution. Integrated intensities were measured at different temperatures with neutrons and X-rays. In this way, anharmonic effects were measured based on neutron diffraction and then their contribution into X-ray scattering was determined. Interestingly, these mechanisms give contributions of opposite sign. Although the anharmonic contribution is usually smaller, it increases with temperature. Diffraction conditions were carefully chosen to avoid possible multiple-diffraction excitations. The values of $F_{\rm Si} = 1.460 \pm 0.007$ and $F_{\rm Ge} = 1.060 \pm 0.009$ for the structure factors at room temperature were reported with the errors determined by mean-square deviations. Since the absolute intensity of the Ge 222 reflection at room temperature was measured relative to the Si 222 reflection, the value of $F_{\rm Ge} = 1.060 \pm 0.05$ was also reported with errors including both statistical

deviations and uncertainty in F_{Si}. This value is close to the value of 1.05 ± 0.08 reported at the same time by Matsushita & Kohra (1974).

Based on the scattering of experimental results for F_{Si} the accuracy of determining the structure factors of the forbidden reflections cannot be considered as very high. Thus, Fujimoto (1974) reported $F_{Si} = 1.51 \pm 0.02$ measured with Ag $K\alpha$ and $F_{Si} = 1.48 \pm 0.02$ with Cu $K\alpha$ based on accurate comparison of 222 and 333 integral intensities. Entin & Smirnova (1989) performed double-crystal 222 rocking-curve measurements in a non-dispersive setup, and from the fit of the rocking curve obtained $F_{Si} = 1.47$. Earlier reported experimental results include $F_{Si} = 1.46 \pm 0.04$ (Roberto & Batterman, 1970), $F_{Si} = 1.44 \pm 0.08$ (DeMarco & Weiss, 1965) and $F_{Si} = 1.48 \pm 0.03$ (Jennings, 1969).

The normal (*i.e.* away from multiple-diffraction conditions) 222 diffraction is very weak and, therefore, kinematical even in perfect crystals. That means that the maximum reflectivity is much less than unity owing to the fact that the extinction length L_{ex} is rather long and much exceeds the absorption length L_a. For example, for a Ge crystal, Cu $K\alpha$ radiation and structure factor $F_{Ge} = 1.060$, we have $L_{ex} = 157$ µm and $L_a = 11$ µm. The situation changes if some other (second) reflection satisfies, even weakly, the Bragg condition near the three-beam diffraction region. This is usually achieved by rotating the crystal azimuthally. Then, the phenomenon of the resonant enhancement of the first reflection by the second one takes place. It was shown by Høier & Marthinsen (1983) mathematically that the effective (two-beam) diffraction parameter for the first reflection in the Bragg condition can be rescaled by the second reflection even if this second reflection is weak (far from the Bragg condition). This is especially important for forbidden reflections because an increased diffraction parameter may change the relation between L_{ex} and L_a and the condition $L_{ex} < L_a$ can be satisfied. If it occurs, then the effect of total reflection for the two-beam forbidden diffraction takes place with a narrow width of the Darwin table (Kohn, 1988). Moreover, the width can be changed by a simple rotation of the crystal over the azimuthal axis.

Although this effect was predicted theoretically many years ago, it was observed experimentally only recently (Kazimirov & Kohn, 2010). This is due to very stringent requirements on monochromatization and collimation of the incident beam. The experiment was performed with a synchrotron beam using multi-crystal post-monochromator optics for additional monochromatization and angular collimation in both vertical and horizontal planes. A maximum 222 reflectivity from an Si crystal of 68% was measured. This work is a continuation of the same experimental approach and here we present results of the 222 Ge measurements. The following section describes the experimental setup and presents an overview of the experimental data. In §3 we discuss the effect of two-wave diffraction into a forbidden direction near the three-beam diffraction condition and the possibility of determining the 222 Ge structure factor. In §4 we analyze the three-beam diffraction angular region and perform a detailed comparison with theory.

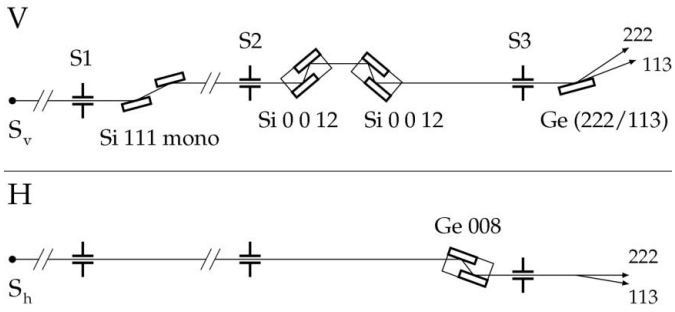

Figure 1
Experiment setup. In the vertical diffraction plane (upper panel) two Si 0,0,12 channel-cut crystals in the dispersive setup were used for additional monochromatization and angular collimation. In the horizontal diffraction plane (lower panel) the beam was collimated with a Ge 008 channel-cut crystal.

2. Experiment

The experiment was performed at the Cornell High Energy Synchrotron Source (CHESS) at the A2 beamline. The X-ray beam from the 49-pole wiggler was monochromated to 24.993 keV with a standard double-crystal Si 111 upstream water-cooled monochromator. Post-monochromator optics for additional monochromatization and angular collimation were assembled on the optical table in the experimental hutch. The sample, a thick Ge (111)-oriented perfect crystal, was mounted on a Huber four-circle diffractometer. The measurements were performed at the ambient temperature in the hutch, 292.0 ± 0.2 K. The diffraction plane for the forbidden 222 reflection was vertical. The 222 and 113 diffracted intensities were recorded as a function of the polar angle θ for various values of the azimuthal angle φ in the vicinity of the three-beam (222/113) diffraction. The experimental setup is shown schematically in Fig. 1. Two diffraction planes, vertical (V) and horizontal (H), are shown in separate panels. The additional monochromatization and collimation over the polar angle was performed with two Si 0,0,12 channel-cut crystals in a dispersive arrangement. The azimuthal angular collimation was achieved with a double-bounce Ge 008 channel-cut crystal diffracted in the horizontal plane. To perform scans with sub-microradian angular steps, additional gear boxes were added to standard Huber gear reducers on both the θ and φ axes.

Experimental θ (polar) angular curves of the intensity of the 113 and 222 beams normalized to the intensity of the incident beam are shown in Figs. 2 and 3, respectively. The curves were measured at different values of the azimuthal angle φ. The exact φ values shown at the left side of each curve were determined by comparison with the theoretical simulations which take into account refraction effects.

The general features of the angular dependences in Figs. 2 and 3 are very similar to the case of silicon which was discussed in detail in our previous work (Kazimirov & Kohn, 2010). The main difference is a much better angular collimation and, therefore, higher resolution which was achieved in the present work. The characteristic drop in 113 intensity predicted by theory at the point of the exact Bragg condition

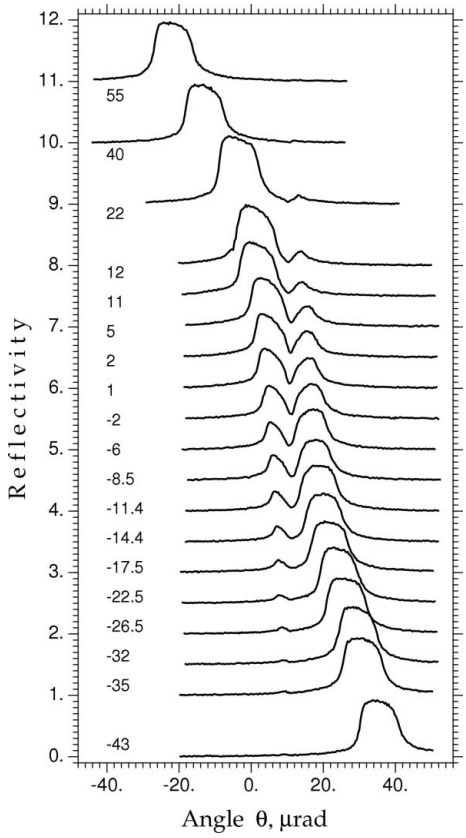

Figure 2
Experimental polar (θ) 113 diffraction profiles. Azimuthal (φ) angles for each curve are shown on the left.

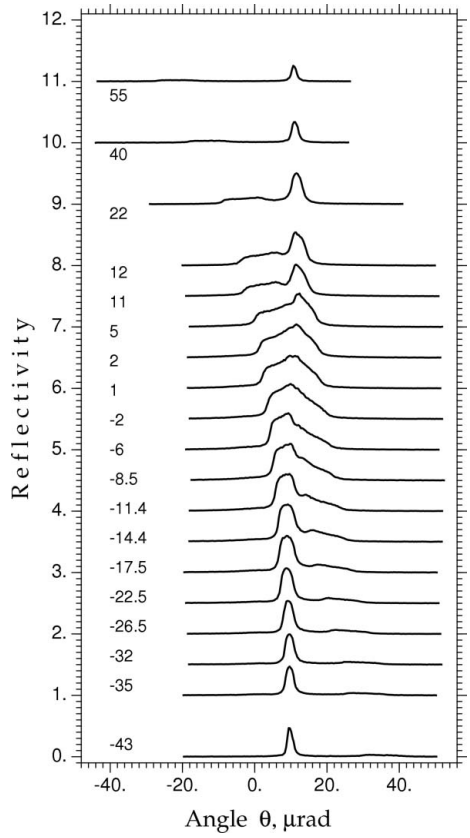

Figure 3
The same as in Fig. 2 but for the 222 reflection.

for the two-beam 222 diffraction is clearly observed. Owing to this effect, the 113 curves in the central part of the three-beam region display a characteristic double-peak shape. The polar curves can be conditionally divided into two parts based on the different physical processes responsible for the excitation of the intensity in three-beam diffraction (Kohn, 1988). The first one is the angular region where the Bragg condition is satisfied for a particular beam. Since the Bragg condition is the condition of resonance, this region is called the resonance part. In the kinematical formula for the wave amplitude this condition leads to a zero value for the denominator. The second part is the region where the Bragg condition is satisfied for the second beam. In this region the kinematical reflectivity has an additional term owing to a two-stage process of diffraction from the second beam. This region is called the amplitude part because the new term appears in the numerator of the kinematical formula.

Of course, the second part exists only near the three-beam region because the denominator increases with increasing angular separation between the two-beam peaks for two reflections. At the large values of the azimuthal angle φ only the two-beam peak which corresponds to the resonant part can be observed on polar curves. However, as clearly seen in Fig. 2, the two-beam peak at the negative values of φ, which is due to the resonant part, continuously transforms into the amplitude part at positive φ values, and *vice versa*. Therefore, the two-beam peaks at negative and positive values of φ are separated by a forbidden zone. A similar effect, as is well known, takes place in the theory of electron or phonon spectra of solids (Kittel, 1963). The physical mechanism responsible for such behavior requires a separate consideration.

Examining the polar curves shown in Fig. 3 one can clearly see that the 222 reflection is symmetric for which the two-beam Bragg condition does not depend on the azimuthal angle. Moreover, the two-beam diffraction is very weak and, therefore, the two-beam peaks are purely resonant in their origin. Indeed, as one can see in the bottom or top curves of Fig. 3, the resonant part of the reflectivity is stronger than the amplitude part, and has a variable width, whereas the amplitude part has the same width as the 113 reflection. Note here that the effect of the total (100%) reflection into the forbidden reflection cannot be observed because germanium strongly absorbs even at a rather high energy of 25 keV and the condition $L_{ex} < L_a$ cannot be satisfied. Nevertheless, the reflectivity close to 60% has been recorded experimentally near the three-beam region. At large values of φ the resonance peak, though semi-kinematical, is rather narrow, with a width which does not depend on φ. We note that such behavior is due to the finite resolution of the experiment.

We want to emphasize that all effects predicted by theory have been observed in this experiment. This was made possible owing to the very high resolution of our experimental setup, though at the expense of photon flux. To estimate the angular resolution of our experimental setup in the vertical plane we measured the two-beam Si 555 rocking curve and

fitted it by performing convolution with the Gaussian function using its width as a fitting parameter. The best fit gives an experimental value of the angular resolution of 0.8 μrad FWHM. This value is significantly higher than the theoretical estimation of about 0.2 μrad of the angular throughput of our multi-crystal setup. Mechanical vibrations in the hutch are most likely the reason for this broadening. The same value of the angular resolution was obtained by fitting Ge 222 rocking curves away from the three-beam diffraction region with the expected (based on the structure factor $F_{\rm Ge}$ = 1.060 discussed above) width of 0.098 μrad. The convolution of the theoretical curves with the Gaussian function with 0.8 μrad FWHM was used for the quantitative comparison of experiment with theory in §4.

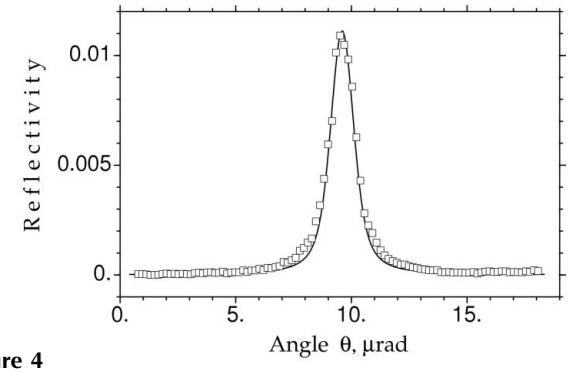

Figure 4
Experimental 222 θ curve measured at $\varphi = -750.5$ μrad (symbols) and the theoretical diffraction peak calculated for $F_{\rm Ge}$ = 1.06 and convoluted with a Gaussian function of width 0.8 μrad (solid line).

3. Forbidden 222 diffraction and the 222 structure factor

The theory of X-ray multiple diffraction in perfect crystals is well known; we refer to our preceding paper (Kazimirov & Kohn, 2010) and references within. Here we want to discuss the far 'wings' of three-beam diffraction intensity when kinematical two-beam diffraction takes place but with a rescaled value of the diffraction parameter. We consider 222 diffraction with the index 1 assigned to the 222 beam and the index 2 assigned to the 113 beam. As was shown, the rescaled scattering amplitude is written as follows,

$$g_{10} = G_{10} + \frac{G_{12}G_{20}}{G_{22}(\varphi)}, \qquad (1)$$

where (neglecting polarization states)

$$G_{mn} = \frac{K\chi_{mn}}{(\gamma_m)^{1/2}(\gamma_n)^{1/2}} - \frac{2\delta_{mn}}{\gamma_m}(\mathbf{h}_m\mathbf{e}_2)\varphi, \qquad K = \frac{2\pi}{\lambda}. \qquad (2)$$

Here λ is the wavelength of the monochromatic radiation, χ_{mn} is a diffraction parameter (Fourier component of the crystal susceptibility) for a reflection from beam n to beam m, δ_{mn} is the Kroneker symbol which is equal to 1 for $m = n$ and 0 in other cases, $\mathbf{h}_m$ is the mth reciprocal lattice vector, γ_n is the cosine of the angle between the nth beam and the internal normal to the entrance surface, and $\mathbf{e}_2$ is the unit vector normal to the direction of the incident beam along which the azimuthal angle is counted. Substituting (2) into (1) we have the following approximate expression for large values of φ,

$$g_{10} = \frac{K}{i(\gamma_0|\gamma_1|)^{1/2}}\left[\chi_{10} + \frac{K}{2(\mathbf{h}_2\mathbf{e}_2)}\frac{\chi_{12}\chi_{20}}{\varphi}\right]. \qquad (3)$$

The second term in the square brackets contains diffraction parameters of allowed strong reflections which are therefore well known. Our goal is to determine the value of χ_{10}, *i.e.* the diffraction parameter for the 222 reflection in the Ge crystal,

$$\chi_{10} = -\frac{\lambda^2 r_0}{\pi V_0}F_{\rm Ge}, \qquad r_0 = \frac{e^2}{mc^2}, \qquad (4)$$

based on the experimental data measured at large φ. Here r_0 is the classical electron radius, e and m are the charge and mass of an electron, respectively, c is the speed of light and V_0 is the volume of the crystal unit cell.

The 222 diffraction profiles were measured for φ values from −750 to 950 μrad. We found that for all φ the width of the θ curves was constant within statistical errors (except, of course, for the central three-beam region where the 222 curves experience dramatic changes). As an example, in Fig. 4 the experimental θ curve measured at $\varphi = -750.5$ μrad is shown (symbols) together with the theoretical diffraction peak calculated for $F_{\rm Ge}$ = 1.06 and convoluted with a Gaussian function of width 0.8 μrad (solid line). All theoretical calculations were performed using a general computer program for the three-beam diffraction which was used in our previous work (Kazimirov & Kohn, 2010). This program is now available online (Kohn, 2011).

The experimental values of the maximum intensity of the 222 diffraction profiles are shown in Fig. 5. They were fitted to the theory using the 222 structure factor as a fitting parameter. The best fit (solid line in Fig. 5) yields a 222 Ge structure factor of $F_{\rm Ge}$ = 1.05, which agrees with the value reported by Matsushita & Kohra (1974) and is close to the value of 1.06 reported by Roberto *et al.* (1974). Note that the φ values are counted from the kinematical Bragg condition which does not

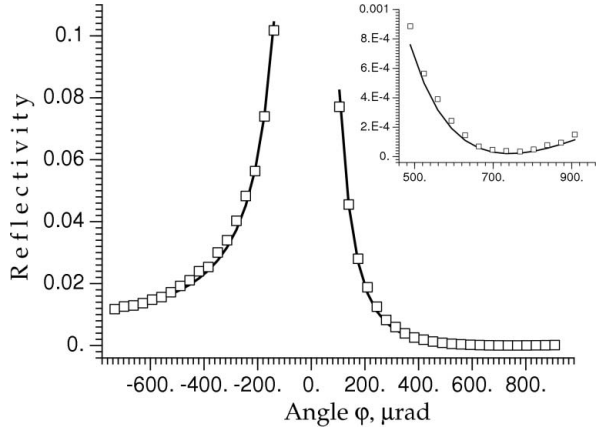

Figure 5
Experimental 222 peak intensities (symbols) and the best fit for the 222 Ge structure factor $F_{\rm Ge}$ = 1.05 (solid line). In the inset the angular region of zero 222 peak intensity is shown.

take into account a shift due to refraction. This is the reason why the center of the three-beam region corresponds to $\varphi \simeq -30$ μrad. This shift is absent in the formula (3). It is very difficult to estimate the accuracy of the structure factor determination for two reasons. First, the peaks at large values of φ are very weak and therefore have rather low statistics. Second, the three-beam calculations are based on known values of the structure factors of other reflections and, as is well known, different databases give slightly different values.

One very interesting feature of the experimental data shown in Fig. 5 is that at certain large and positive φ values the intensity of the 222 diffraction peak is zero, *i.e.* the peak is below the detection limit. This is clearly seen in the inset of Fig. 5. This may only occur if the scattering amplitude (3) becomes zero. Since the quantities χ_{nm} are complex, this means that the phase ϕ_{10} of complex value χ_{10} is equal to the sum of phases $\phi_{12} + \phi_{20}$ of χ_{12} and χ_{20} or may differ only by π. This is consistent with the conclusion made by Post & Ladell (1987). We note that the calculations were performed in the coordinate system with the origin at the node of the crystal lattice. However, if one chooses the origin of the Ge unit cell in the inversion center, then all structure factors become real. Therefore in the base coordinate system the phase $\phi_{nm} = -\mathbf{h}_{nm}\boldsymbol{\rho} \pm \pi s$ for all allowed reflections, where $\boldsymbol{\rho}$ is the radius vector of the inversion center, and s equals 1 if $\cos(\mathbf{h}_{nm}\boldsymbol{\rho}) < 1$ and 0 in the opposite case. In our calculations we apply $\phi_{12} = \phi_{20} = -\pi/4$, $\phi_{10} = \pi/2$, so that $\phi_{10} - \phi_{12} - \phi_{20} = \pi$. Thus, the 222 structure factor is purely imaginary, a fact which has not been reported in the works discussed above. We note that the $\pi/2$ value of the structure factor phase does not mean absorption; it only means a complex behavior of the asymmetric electron-density distribution.

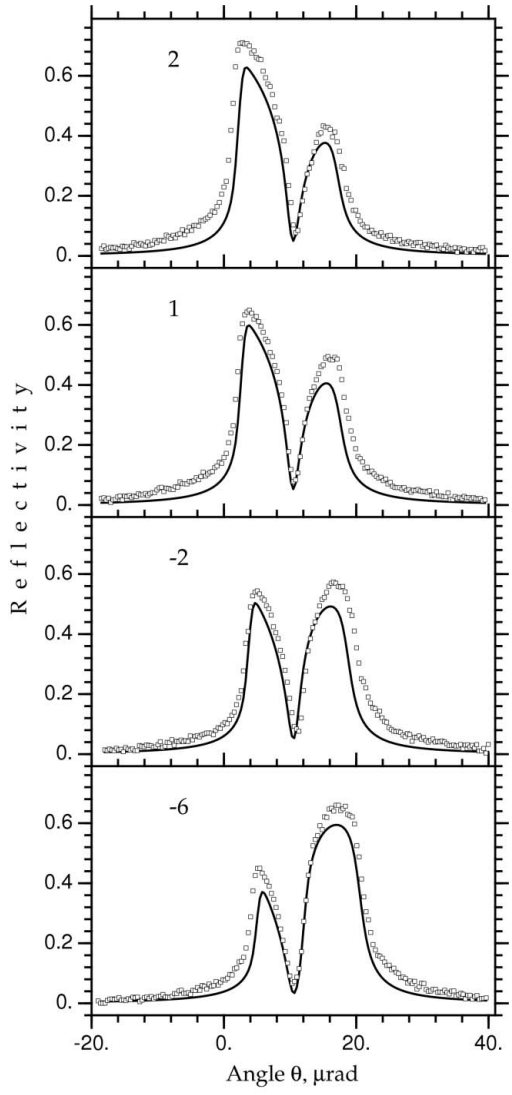

Figure 6
Comparison of the experimental polar scans (symbols) for the 113 reflection with computer simulations (solid lines).

4. Computer simulations and comparison with experimental data

In this section we want to discuss in detail the agreement between the measured polar scans and computer simulations inside the strong dynamical three-wave diffraction region of width only a few arcseconds in both θ and φ. The problems of mechanical stability and reproducibility are the main experimental issues in performing scans with sub-microradian steps. Because the absolute values of the polar angle relative to the exact kinematical three-wave point cannot be determined experimentally, the origin of the θ scale was used as a free fitting parameter. The total θ range for each scan was fixed to its experimental value, *i.e.* the experimental value of the angular step size was used in simulations. The azimuthal angle φ was also considered as an independent free parameter and it was determined from the best agreement between the computer simulations and the experiment for each individual scan. The theoretical curves were calculated by summing up the curves calculated for the plane wave within the azimuthal angular range of 4 μrad and then performing the convolution over the θ angle with a Gaussian function of 0.8 μrad FWHM.

Fig. 6 shows four 113 experimental curves (symbols) in the central three-beam region and their theoretical simulations (solid lines). The values of the azimuthal angle φ in microradians are shown on the left side of each curve. Fig. 7 shows the 222 curves for the same azimuthal angles. Both the 113 and 222 intensities were measured simultaneously by two different scintillation detectors. Both intensities were normalized to the same value of the incident beam intensity. As one can see in Fig. 7, the absolute values of the 222 reflection coefficient as well as the shapes of the curves agree with the computer simulations remarkably well. This is not quite the case for the 113 beam in Fig. 6; the experimental curves are slightly wider and the absolute values of the reflection coefficient are slightly higher than theory. One of the factors that may contribute to this discrepancy is possibly a small difference in efficiency between different types of scintillation detectors.

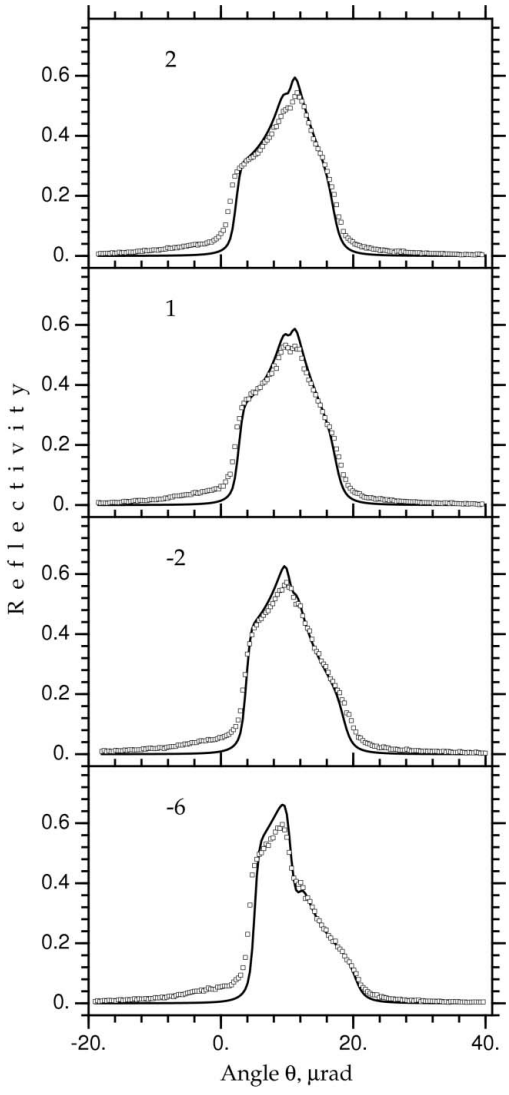

Figure 7
The same as in Fig. 6 but for the 222 reflection.

In general, the agreement between theoretical and experimental curves is extremely good. In dynamical two-beam diffraction such agreement between theory and experiment can no longer surprise anyone and any possible discrepancy is usually attributed to crystal imperfections. Here, in fact, for the first time such agreement between theory and experiment was achieved in the field of dynamical multiple diffraction. The detailed analysis became possible owing to the high degree of angular collimation and the monochromatization of the incident beam which was achieved by using additional X-ray optics. Such a degree of high angular collimation of only a few microradians in both vertical and horizontal planes will be the standard feature of the next generation of X-ray sources such as X-ray free-electron lasers and energy-recovery linacs, making possible utilization of a rich variety of multiple-diffraction effects in the next generation of X-ray crystal optics.

This work is based upon research conducted at the Cornell High Energy Synchrotron Source (CHESS) which is supported by the National Science Foundation and the National Institutes of Health/National Institute of General Medical Sciences under NSF award DMR-0936384. The work of VGK was supported by RFBR grant No. 1002-00047-a.

References

Authier, A. (2005). *Dynamical Theory of X-ray Diffraction*, 3rd ed. Oxford University Press.
Chang, S.-L. (2004). *X-ray Multiple-Wave Diffraction: Theory and Application*, *Springer Series in Solid-State Sciences*. Berlin: Springer.
Colella, R. (1974). *Acta Cryst.* A**30**, 413–423.
DeMarco, J. J. & Weiss, R. J. (1965). *Phys. Rev. A*, **137**, 1869–1871.
Entin, I. R. & Smirnova, I. A. (1989). *Acta Cryst.* A**45**, 577–580.
Fujimoto, I. (1974). *Phys. Rev. B*, **9**, 591–599.
Høier, R. & Marthinsen, K. (1983). *Acta Cryst.* A**39**, 854–860.
Jennings, L. D. (1969). *J. Appl. Phys.* **40**, 5038.
Kazimirov, A. & Kohn, V. G. (2010). *Acta Cryst.* A**66**, 451–457.
Kittel, C. (1963). *Quantum Theory of Solids.* New York: Wiley.
Kohn, V. G. (1988). *Kristallografiya*, **33**, 567–573.
Kohn, V. G. (2011). *Online computer program for the three-wave diffraction*, http://xray-optics.ucoz.ru/editor.htm.
Matsushita, T. & Kohra, K. (1974). *Phys. Status Solidi*, **24**, 531–541.
Post, B. & Ladell, J. (1987). *Acta Cryst.* A**43**, 173–179.
Renninger, M. (1937). *Z. Naturwiss.* **25**, 43.
Roberto, J. B. & Batterman, B. W. (1970). *Phys. Rev. B*, **2**, 3220.
Roberto, J. B., Batterman, W. & Keating, D. T. (1974). *Phys. Rev. B*, **9**, 2590–2599.